



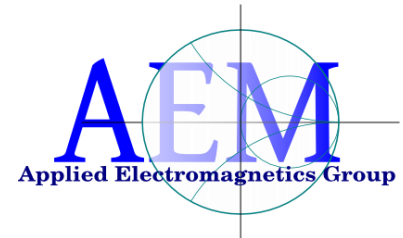
DITEN



URSI GASS 2020

Rome, Italy

29 August - 5 September 2020



A Microwave Diagnostic Technique for Early-Stage Brain Stroke Characterization

A. Fedeli, A. Randazzo, A. Sciarrone, I. Bisio, F. Lavagetto, and M. Pastorino

Department of Electrical, Electronic, Telecommunications Engineering and Naval Architecture (DITEN) – University of Genoa, Italy





Introduction

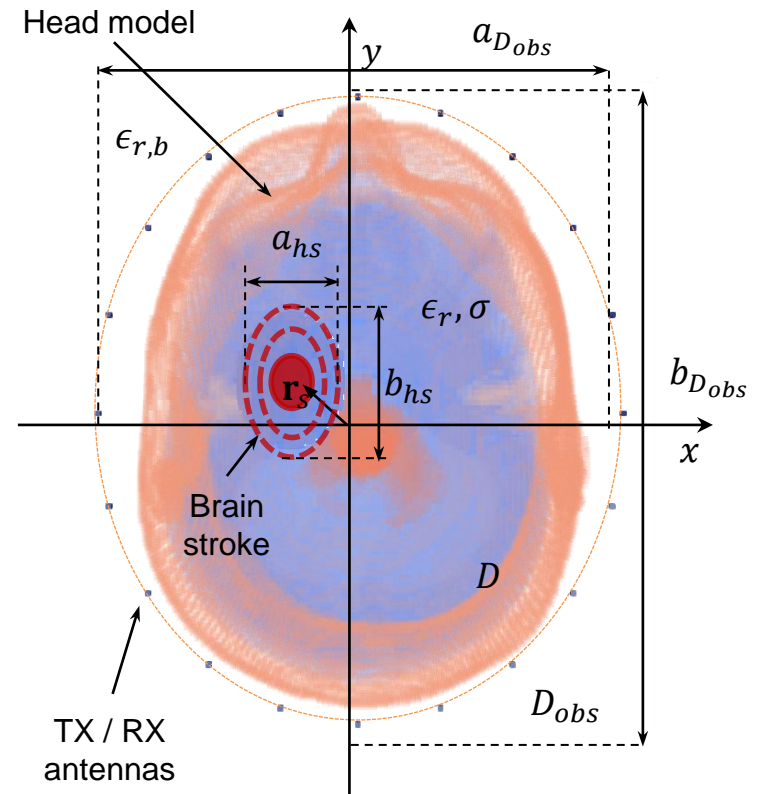
- ❑ **Brain stroke** is well known as one of the leading causes of death and disability worldwide.
- ❑ Within **electromagnetic diagnostic techniques** [1, 2] an increasing interest is attracted by **brain stroke detection** [3 – 6].
- ❑ A novel **tomographic multistatic system** where the acquired data are processed by an **inexact Newton** scheme in **variable-exponent L^p spaces** is presented.
- ❑ **Simulated and experimental results** are shown.

- [1] J.-C. Bolomey, “Advancing Microwave-Based Imaging Techniques for Medical Applications in the Wake of the 5G Revolution,” in **2019 13th European Conference on Antennas and Propagation (EuCAP), 2019**, pp. 1–5.
- [2] O. M. Bucci, G. Bellizzi, S. Costanzo, L. Crocco, G. Di Massa, and R. Scapaticci, “Assessing detection limits in magnetic nanoparticle enhanced microwave imaging,” **IEEE Access**, vol. 6, pp. 43192–43202, 2018.
- [3] A. E. Stancombe, K. S. Bialkowski, and A. M. Abbosh, “Portable microwave head imaging system using software-defined radio and switching network,” **IEEE J. Electromagn. RF Microw. Med. Biol.**, 3, 4, Dec. 2019, pp. 284–291.
- [4] V. L. Coli, P.-H. Tournier, V. Dolean, I. E. Kanfoud, C. Pichot, C. Migliaccio, and L. Blanc-Féraud, “Detection of simulated brain strokes using microwave tomography,” **IEEE J. Electromagn. RF Microw. Med. Biol.**, 3, 4, Dec. 2019, pp. 254–260.
- [5] R. Scapaticci, J. Tobon, G. Bellizzi, F. Vipiana, and L. Crocco, “Design and numerical characterization of a low-complexity microwave device for brain stroke monitoring,” **IEEE Trans. Antennas Propag.**, 66, 12, Dec. 2018, pp. 7328–7338.
- [6] L. Crocco, I. Karanasiou, M. James, and R. C. Conceição, Eds., **Emerging electromagnetic technologies for brain diseases diagnostics, monitoring and therapy**. Springer International Publishing, 2018.

Inverse problem configuration & assumptions

- A **simplified 2D scalar model** with dielectric properties independent from the axial coordinate z has been assumed [1]
- The head, located in a known investigation domain D , is illuminated by a known time-harmonic TM_z incident electromagnetic field e_{inc}
- Head is surrounded by a lossy **coupling medium** with complex dielectric permittivity ϵ_b
- Estimation of the **reference dielectric profile** of the head characterized by a contrast function $\tilde{c} = (\tilde{\epsilon} - \epsilon_b) / \epsilon_b$ ($\tilde{\epsilon}$ being the complex dielectric permittivity of the reference profile)

Configuration of the considered model and measurement system



[1] I. Bisio, C. Estatico, A. Fedeli, F. Lavagetto, M. Pastorino, A. Randazzo, and A. Sciarrone, "Variable-exponent Lebesgue-space inversion for brain stroke microwave imaging," *IEEE Transactions on Microwave Theory and Techniques*, vol. 68, no. 5, pp. 1882–1895, May 2020. <https://doi.org/10.1109/TMTT.2019.2963870>.

Inverse scattering problem formulation

- The scattering problem is formulated as

$$\begin{cases}
 \Delta e(\mathbf{r}) = -k_b^2 \int_{D_{inv}} x(\mathbf{r}') e_{tot}(\mathbf{r}') g(\mathbf{r}, \mathbf{r}') d\mathbf{r}', & \mathbf{r} \in \mathcal{M} \\
 e_{tot}(\mathbf{r}) = e_{ref}(\mathbf{r}) - k_b^2 \int_{D_{inv}} x(\mathbf{r}') e_{tot}(\mathbf{r}') g(\mathbf{r}, \mathbf{r}') d\mathbf{r}', & \mathbf{r} \in \mathcal{D}
 \end{cases}$$

Scattered field $\Delta e(\mathbf{r})$ (orange box)
 Total field $e_{tot}(\mathbf{r})$ (yellow box)
 Reference field due to c_{ref} $e_{ref}(\mathbf{r})$ (purple box)
 Differential contrast function $x(\mathbf{r}') = c(\mathbf{r}') - c_{ref}(\mathbf{r}')$ (red box)
 Green's function $g(\mathbf{r}, \mathbf{r}')$ (green box)

$G_{data} x e_{tot}$ (red arrow)
 $G_{state} x e_{tot}$ (green arrow)

where

- $c = (\epsilon - \epsilon_b)/\epsilon_b$ is the contrast function of the actual configuration (which gives rise to the field e_{tot})
 - $c_{ref} = (\epsilon_{ref} - \epsilon_b)/\epsilon_b$ represent the contrast function of the reference configuration (related to the field e_{ref})
- By **combining** the two equations, we obtain the **scattering model**

$$\Delta e(\mathbf{r}) = F(x)(\mathbf{r}) = G_{data} x (I - G_{state} x)^{-1} e_{ref}(\mathbf{r})$$



Inversion procedure

- To solve this nonlinear equation, an **inexact-Newton** iterative method is applied to **minimize the residual functional** $\Psi: X \rightarrow \mathbb{R}$

$$\Psi(x) = \frac{1}{2} \|F(x) - \Delta e\|_Y^2,$$

where $x \in X$, $\Delta e \in Y$, $F: X \rightarrow Y$, and $\|\cdot\|_Y^2$ denotes the square of the norm of the functional space Y

- In particular, **variable exponent Lebesgue spaces** $L^{p(\cdot)}$ [3] are considered, in which the **power** p used in the norm is **not constant**, but it is a **function** $p(\cdot)$.

[3] C. Estatico, A. Fedeli, M. Pastorino, and A. Randazzo, "Quantitative microwave imaging method in Lebesgue spaces with nonconstant exponents," *IEEE Trans. Antennas Propag.*, vol. 66, no. 12, pp. 7282–7294, Dec. 2018.



Inversion procedure

- The exponent function for the space of the unknowns X depends upon the position inside the investigation domain, allowing to set different values of the parameter p to each point.
- The function $p(\mathbf{r})$ is updated at each step as

$$p_k(\cdot) = p_{min} + (p_{max} - p_{min}) |x_k| / \max_D |x_k|$$

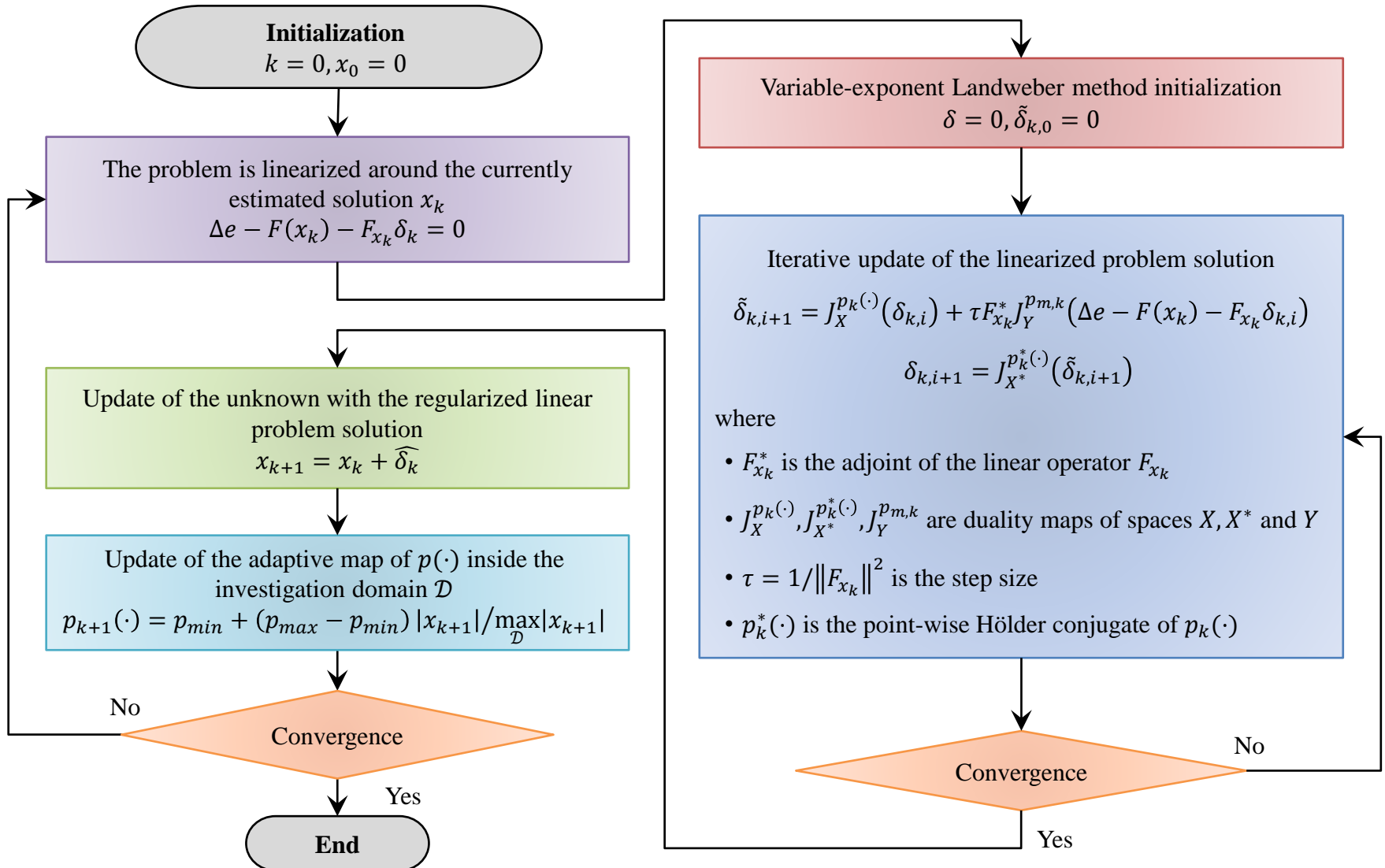
- Two possible initializations are considered:

- A fixed value is used, i.e., $p_0(\mathbf{r}) = p_{start}$
- A delay-and-sum qualitative scheme is used to build the initial map, i.e.,

$$I(\mathbf{r}) = \int_M \int_{\Omega} E_s(\mathbf{r}', \omega) e^{j\frac{2\omega}{v}\|\mathbf{r}-\mathbf{r}'\|} d\omega d\mathbf{r}' \rightarrow p_0(\mathbf{r}) = p_{min} + (p_{max} - p_{min}) \frac{|I(\mathbf{r})|}{\max_{\mathbf{r} \in D} |I(\mathbf{r})|}$$



Inversion procedure

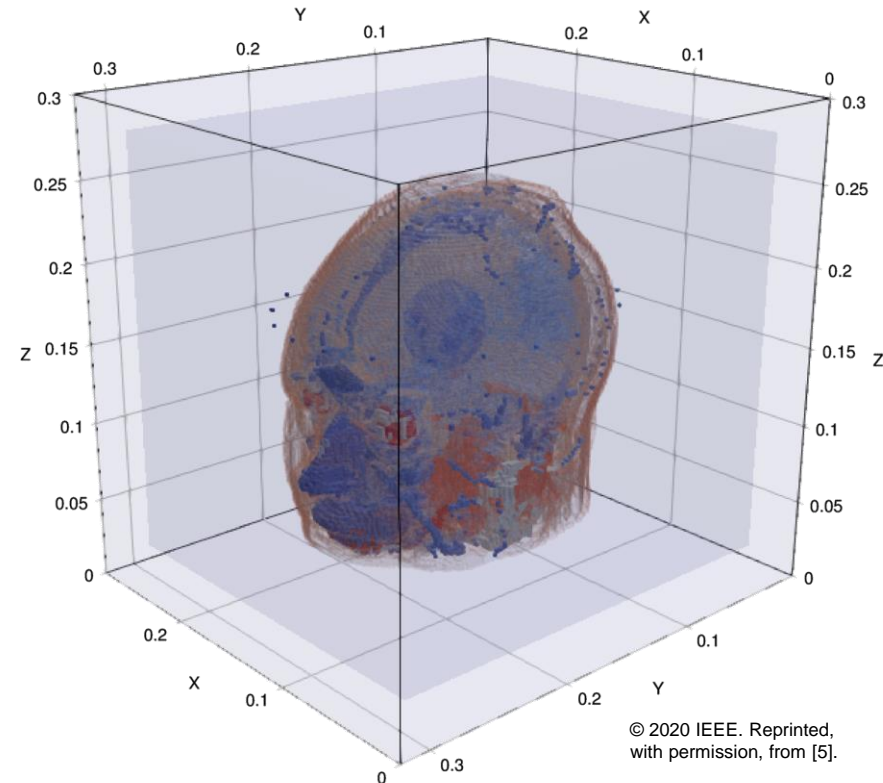


Brain stroke detection – Numerical results

Three-dimensional FDTD simulation domain

Simulation parameters

- ❑ Head of the *AustinWoman 3D model* [1] with 2-mm voxel size
- ❑ Time-domain forward simulation by using *gprMax FDTD* [2]
- ❑ Dispersive **tissue properties** [3, 4]
- ❑ Domain **size**: $28.4 \times 32 \times 30$ cm (3.4×10^6 cells of 2 mm side)
- ❑ **PML** boundary (10 cells)
- ❑ Time step: 3.85×10^{-12} s
- ❑ Time window: 3×10^{-8} s
- ❑ $S = 21$ **antennas** (Hertzian dipoles) on an ellipse of semi-axes 9.2 cm and 11 cm.
- ❑ Excitation signal: Gaussian derivative centered at 1 GHz
- ❑ Background **coupling medium**: glycerin/water mixture 70%
- ❑ Scattered field data corrupted by additive white Gaussian noise with $SNR = 25$ dB.



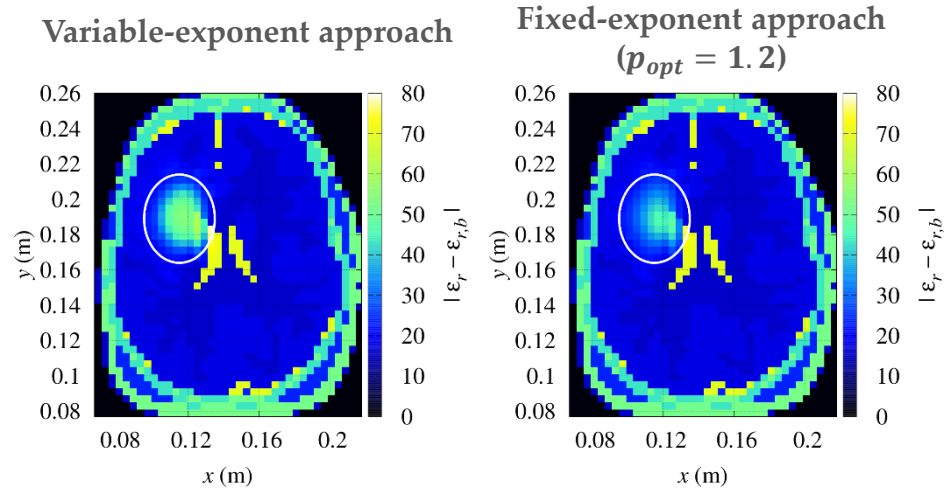
- [1] J. W. Massey et al., *38th Ann. Int. Conf. of the IEEE EMBS*, 2016.
- [2] C. Warren et al., *Comput. Physics Comm.*, 209, 2016.
- [3] J. M. Fujii, *IEEE MWCL*, 22, (2), 2012.
- [4] S. Mustafa et al., *IEEE TAP*, 62 (3), 2014.
- [5] I. Bisio, C. Estatico, A. Fedeli, F. Lavagetto, M. Pastorino, A. Randazzo, and A. Sciarrone, "Variable-exponent Lebesgue-space inversion for brain stroke microwave imaging," *IEEE TMTT*, 68(5), 2020.

Brain stroke detection – Numerical results

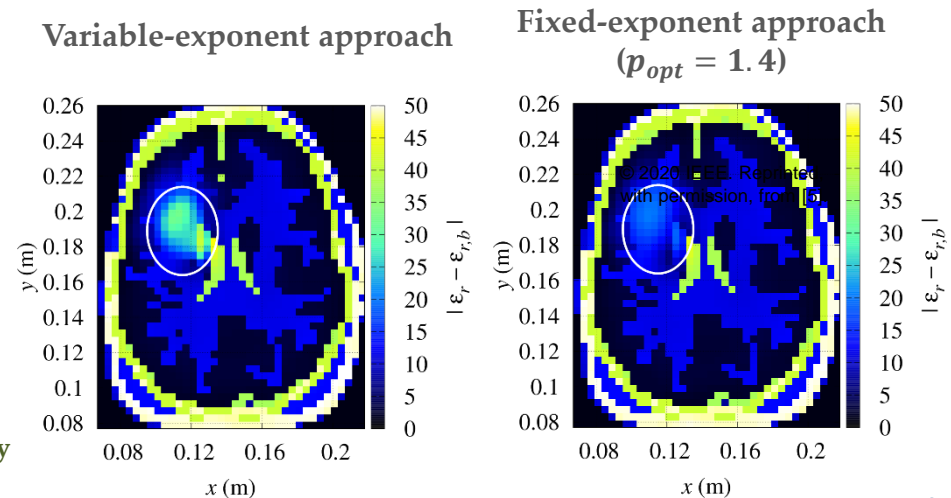
Measurement configuration

- ❑ Ellipsoidal inclusion:
hemorrhagic brain stroke at (11.7, 17.2, 17.5) cm
- ❑ **Healthy head profile** used as reference model
- ❑ Investigation domain composed by 1485 cells with 4 mm side
- ❑ Frequency hopping started from 500 Mhz and with step 50 MHz.
- ❑ Range of values of the exponent function: [1.4,2].
- ❑ Initial exponent map: constant value equal to 1.4.

Reconstructed dielectric properties at 0.5 GHz



Reconstructed dielectric properties at 0.8 GHz



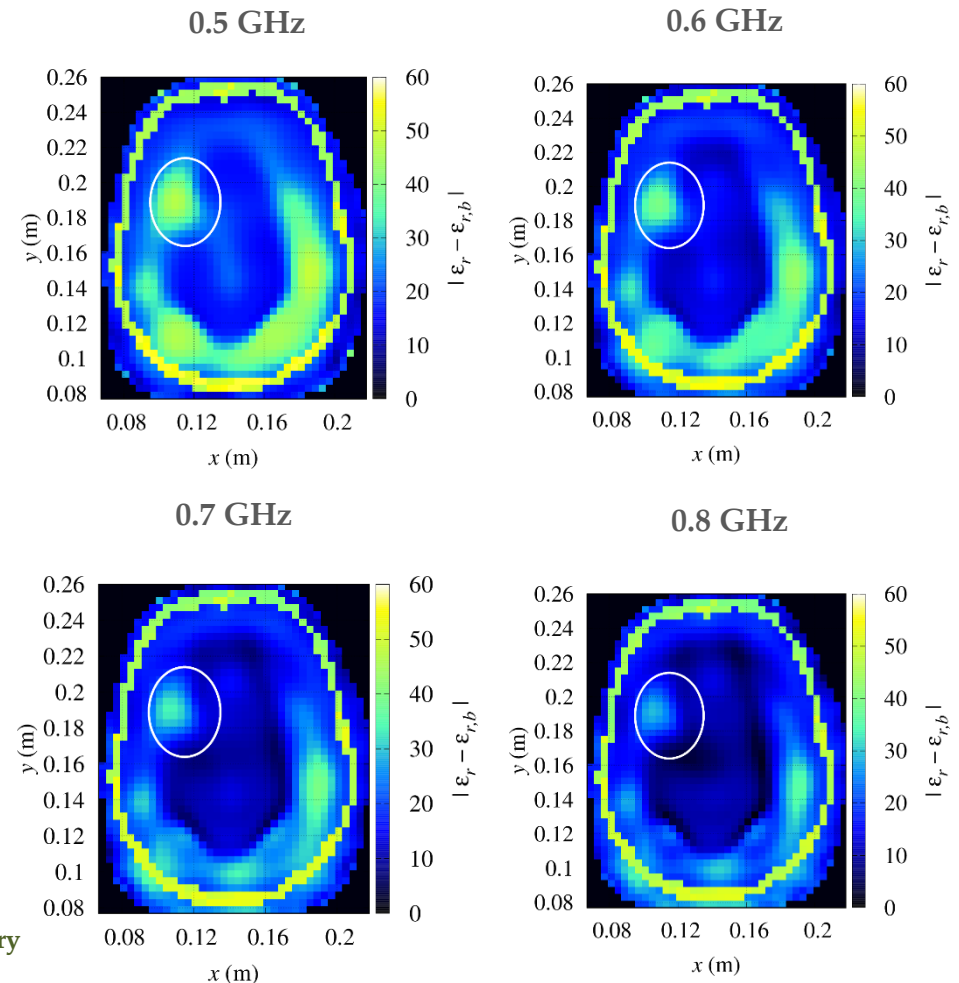
[1] I. Bisio et al., "Variable-exponent Lebesgue-space inversion for brain stroke microwave imaging," *IEEE Transactions on Microwave Theory and Techniques*, vol. 68, no. 5, pp. 1882–1895, May 2020.

Brain stroke detection – Numerical results

Measurement configuration

- ❑ Ellipsoidal inclusion:
hemorrhagic brain stroke at (11.7, 17.2, 17.5) cm
- ❑ **Partially homogeneous configuration** (except skull) used as reference model
- ❑ Investigation domain composed by 1485 cells with 4 mm side
- ❑ Frequency hopping started from 500 Mhz and with step 50 MHz.
- ❑ Range of values of the exponent function: [1.4,2].
- ❑ Initial exponent map: constant value equal to 1.4.

Reconstructed dielectric properties (variable exponent approach)



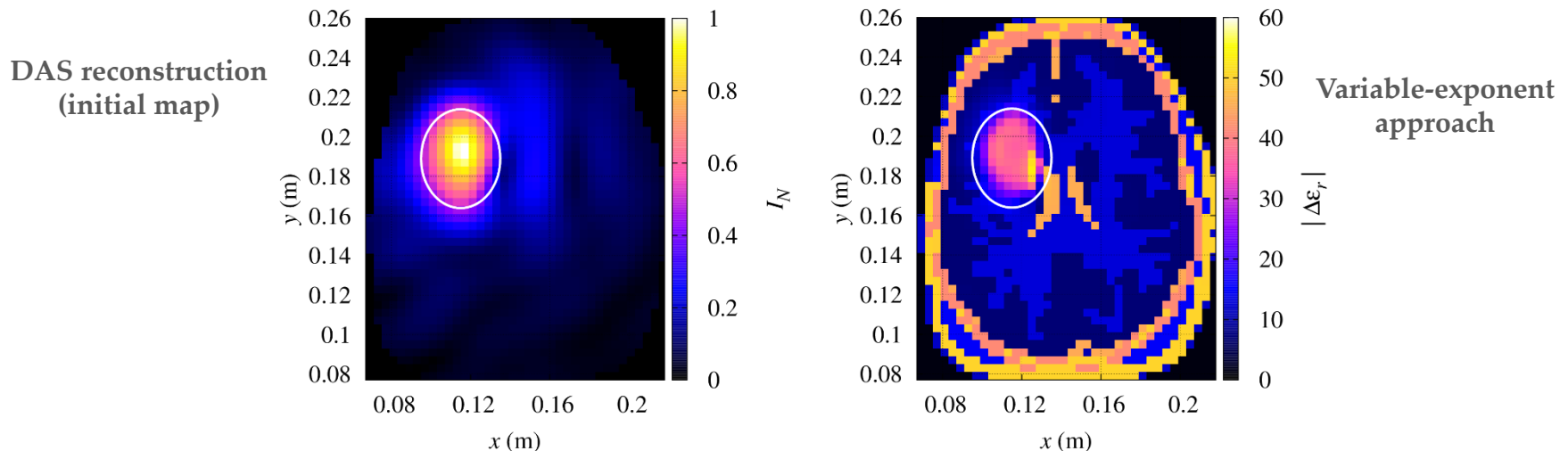
[1] I. Bisio et al., "Variable-exponent Lebesgue-space inversion for brain stroke microwave imaging," *IEEE Transactions on Microwave Theory and Techniques*, vol. 68, no. 5, pp. 1882–1895, May 2020.

Brain stroke detection – Numerical results

Measurement configuration

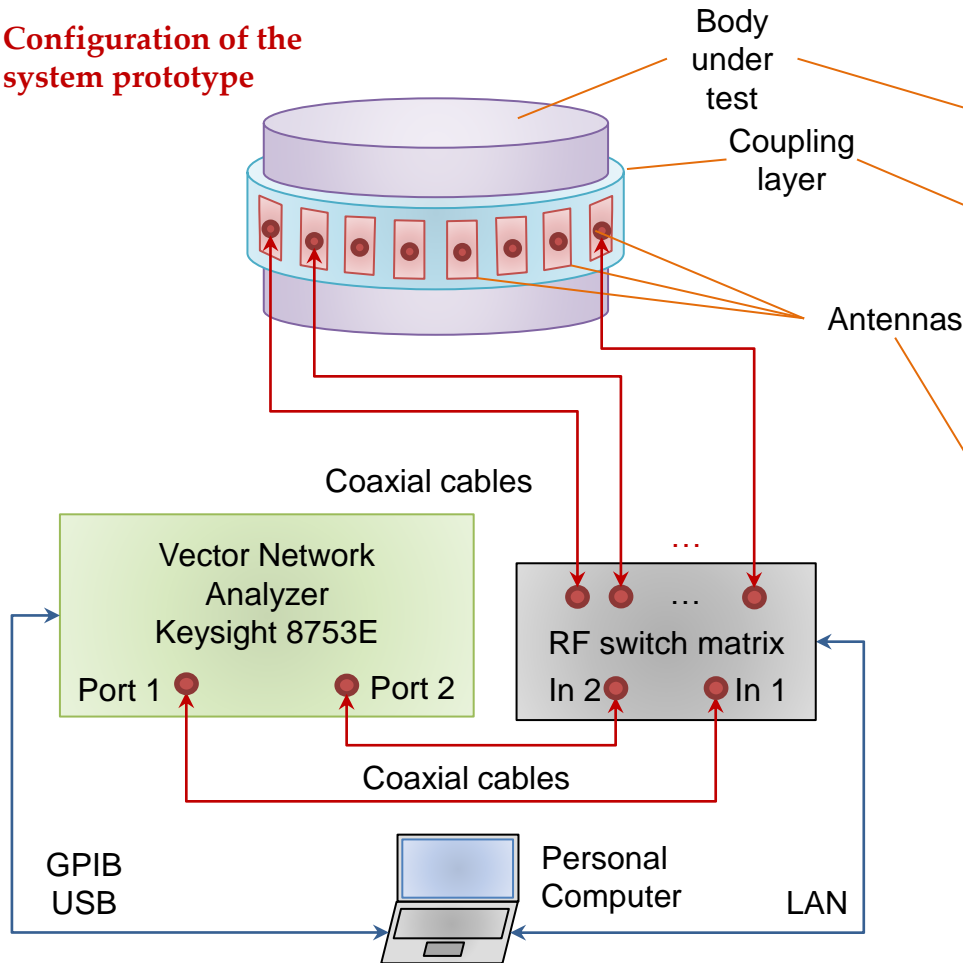
- ❑ Ellipsoidal inclusion: **hemorrhagic brain stroke** at (11.7, 17.2, 17.5) cm
- ❑ **Healthy head profile** used as reference model
- ❑ Investigation domain composed by 1485 cells with 4 mm side
- ❑ Frequency hopping started from 500 MHz and with step 50 MHz.
- ❑ Range of values of the exponent function: [1.4,2].
- ❑ Initial exponent map: **obtained by applying the DAS scheme.**

Reconstructed dielectric properties at 0.7 GHz

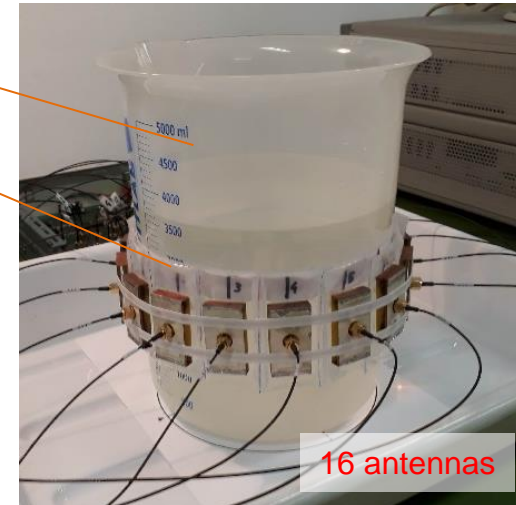


Brain stroke detection – Experimental results

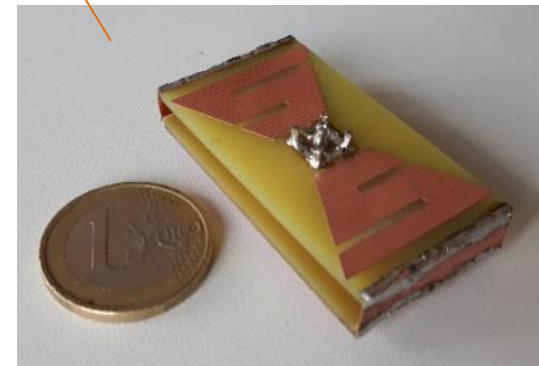
Configuration of the system prototype



Cylindrical test target



Bowtie-like antenna structure [1]



[1] I. Bisio et al., "Brain stroke microwave imaging by means of a Newton-conjugate-gradient method in L_p Banach spaces," *IEEE Transactions on Microwave Theory and Techniques*, vol. 66, no. 8, pp. 3668–3682, Aug. 2018.

Preliminary experimental results

□ Target properties

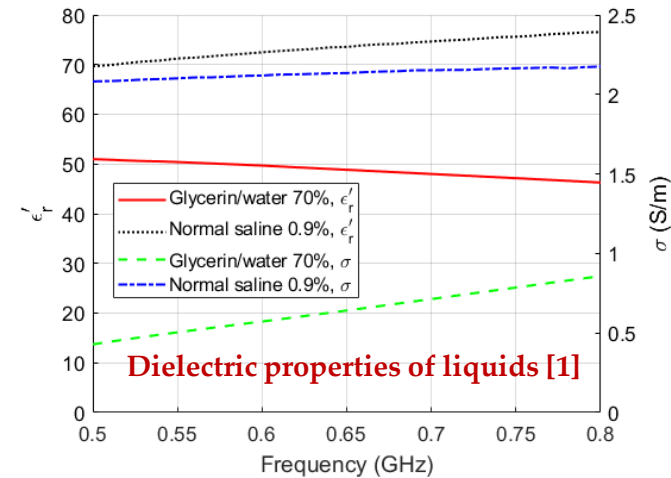
- **Outer structure** (filled with 70% glycerin/water mixture)
 - 5 L PP beaker (external diameter of 180 mm, 4 mm thickness) filled with 70% glycerin/water mixture
- **Cylindrical inclusions** (filled with 0.9% saline solution)
 - 100 mL PP circular cylinder, 20 mm diameter
 - 500 mL PP circular cylinder, 52 mm diameter

□ Configuration parameters

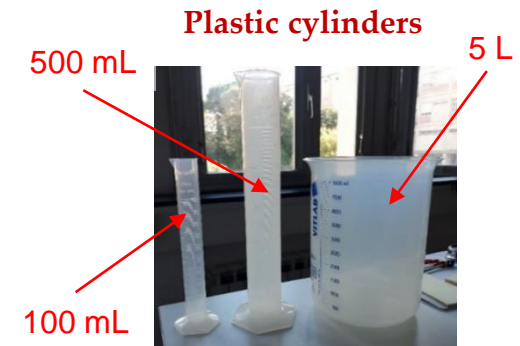
- Coupling medium (70% glycerin/water mixture) in **PE bags** (40 x 80 mm, 100 μm thick, 20 ml volume) around the outer cylinder
- Investigation domain partitioned into $N_i = 1264$ square cells of side $d_i = 4.5$ mm

□ Parameters of the inverse solver

- $p_{start} = p_{min} = 1.4, p_{max} = 2.0$
- Number of maximum allowed inner and outer iterations to $N_{IN} = N_{LW} = 100$, minimum residual variation $r_{IN} = r_{LW} = 0.35$



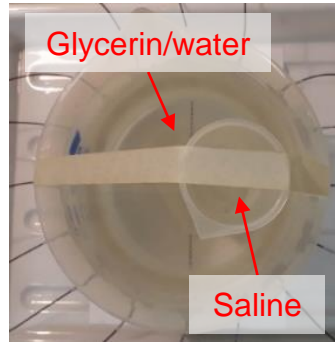
© 2020 IEEE. Reprinted, with permission, from [1].





Preliminary experimental results

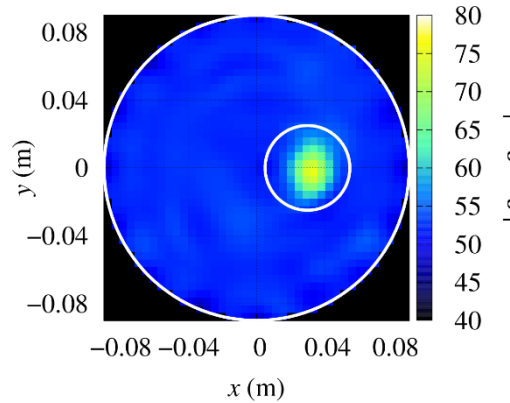
Target configuration – Single circular inclusion (\varnothing 52 mm cylindrical inclusion)



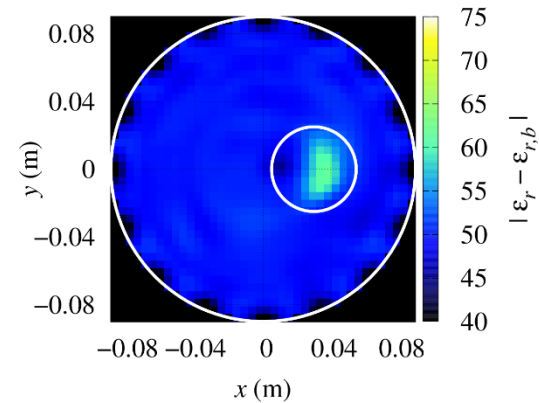
© 2020 IEEE. Reprinted, with permission, from [1].

Reconstructed relative dielectric properties (variable exponent)

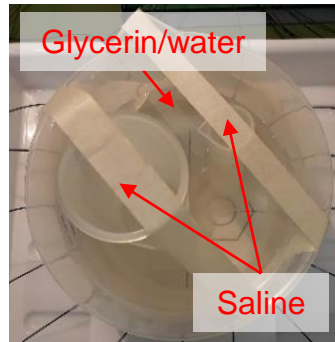
$f = 600$ MHz



$f = 900$ MHz



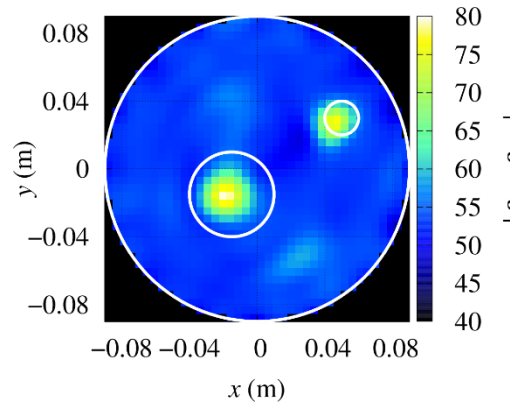
Target configuration – Two circular inclusions (\varnothing 20 mm and \varnothing 52 mm cylindrical inclusions)



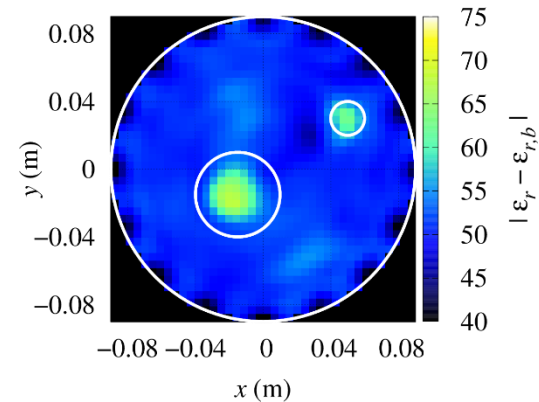
© 2020 IEEE. Reprinted, with permission, from [1].

Reconstructed relative dielectric properties (variable exponent)

$f = 600$ MHz



$f = 900$ MHz



[1] I. Bisio, C. Estatico, A. Fedeli, F. Lavagetto, M. Pastorino, A. Randazzo, and A. Sciarrone, "Variable-exponent Lebesgue-space inversion for brain stroke microwave imaging," *IEEE Transactions on Microwave Theory and Techniques*, vol. 68, no. 5, pp. 1882–1895, May 2020.



Conclusions

- ❑ A novel **tomographic multistatic microwave imaging system** for **brain stroke detection** has been designed
- ❑ A **variable-exponent Lebesgue-space inversion** scheme is adopted for processing the acquired data.
- ❑ Two initialization strategies have been considered:
 - Constant exponent function
 - Variable exponent function obtained by a delay-and-sum scheme.
- ❑ Numerical **simulations** and preliminary **experimental results** have been carried out
- ❑ **Further activities** will be devoted to
 - Improve the measurement system
 - Test the method in more realistic configurations, also with clinical data